

E-9-8L

A Quantum Dot Swept Laser Source Based Upon a Multi Section Laser Device

B.J. Stevens, D.T.D Childs, K.M. Groom, M. Hopkinson and R.A. Hogg

EPSRC National Centre for III-V Technologies, Department of Electronic and Electrical Engineering, University of Sheffield, Mappin Street, Sheffield S1 3JD, UK.

There is currently a large research effort to develop light sources for medical imaging applications, such as optical coherence tomography (OCT). OCT is a 3D imaging technique based upon white light interferometry which enables *in-situ* imaging of living cells. Wavelengths for imaging skin tissue are either 1050nm (zero dispersion in aqueous tissue e.g. the eye) or 1300nm (minimum absorption and scattering in the skin) [1]. Swept source (SS)-OCT offers a 20-30dB sensitivity advantage over time domain (TD)-OCT which enables real time (30fps) imaging. [2]

Current swept laser sources (SLS) are based upon external piezo-electric mechanically swept gratings or mirrors, limiting sweep speed to ~20KHz [3,4] but delivering 170pm linewidth and a >100nm sweep range. Monolithic integration of semiconductor gain medium and a grating is limited in sweep range due to the refractive index change, although approaches such as the SSG-DBR have extended the sweep range [5].

Quantum Dot (QD) based laser have demonstrated low threshold current [6] and temperature invariant operation [7], both of which are advantageous for laser operation. Self assembled QDs have broad gain spectra due to the inhomogeneous broadening, which can limit the maximum gain achievable, but for our device this is an advantage.

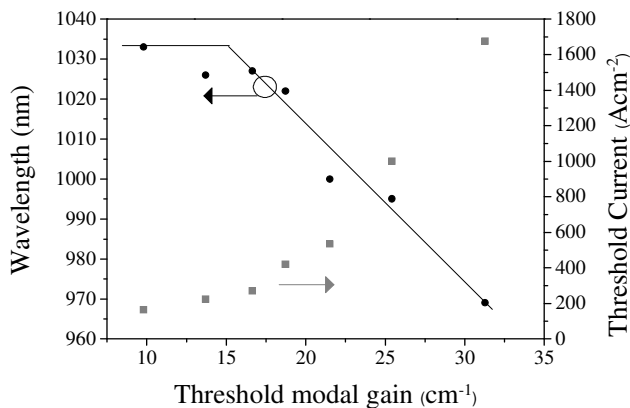


Figure 1. Lasing wavelength and threshold current density as a function of threshold modal gain for 50μm broad area lasers.

The sample was grown by solid source MBE in a Semicon V90H reactor on Si doped GaAs substrate. A QD active region consisting of 5 repeats of 2.5nm GaAs, InAs QDs, 2.5nm GaAs and 7nm Al_{0.15}Ga_{0.85}As, was grown inside an optical waveguide structure.

Broad area lasers were fabricated. Length dependent characterisation (for lengths >1.5mm) gives the internal quantum efficiency $\eta_i = 57 \pm 5\%$, transparency current density $J_0 = 45 \pm 5 \text{ Acm}^{-2}$ and the internal loss $\alpha_i = 2.0 \pm 2 \text{ cm}^{-1}$. For cavity lengths shorter than 1.5mm nonlinearity in the length dependent characterisation is observed due to incomplete gain clamping (population of the excited states (ES)).

Figure 1 presents the lasing wavelength and threshold current density as a function of the threshold modal gain. A change of lasing wavelength of >60nm is observed and it is this behaviour that provides the basis for our proposed and demonstrated SLS.

A multisection device was fabricated with section lengths of 500 μm and 250 μm , termed long and short respectively. The device had a wet etched 5 μm ridge and the resistance between adjacent sections was $\sim 1\text{k}\Omega$. The device is shown schematically in the inset to figure 2. With equal current densities in both sections the device behaves as if it was a single contact laser and lases at 1029 nm. When the current densities in the two sections are different, one section can be considered to alter the gain required in the other section in order to achieve lasing. As can be seen from figure 1 the lasing wavelength is a function of the threshold modal gain, hence by varying the ratio of injected currents into the two sections it is possible to sweep the lasing wavelength.

Figure 2 shows the lasing wavelength as a function of the current injected into the two sections. Continuous tuning is achieved over almost 12 nm with the total sweep extending to 25 nm. Lasing is not observed between 1017.4 nm and 1007.9 nm which we believe is due to the peak of the gain spectra not changing continuously with current. Figure 3 shows normalised lasing spectra for the device over the region where continuous tuning is demonstrated. The linewidth is $<125\text{pm}$ which is suitable for OCT applications.

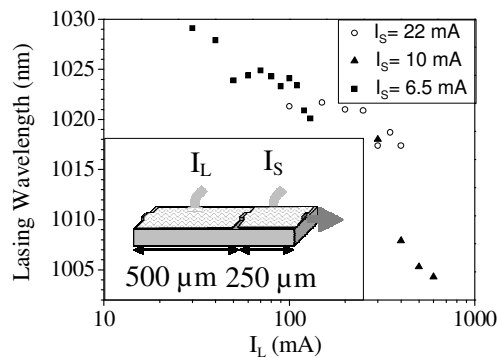


Figure 2. Lasing wavelength as a function of current through the two sections. Inset is a schematic of the device.

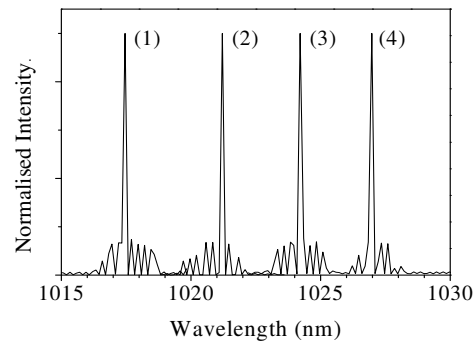


Figure 3. Normalised representative lasing spectra for the device. 1). $I_S=10\text{ mA}$, $I_L=400\text{ mA}$, 2) $I_S=9\text{ mA}$, $I_L=250\text{ mA}$ 3) $I_S=22\text{ mA}$, $I_L=100\text{ mA}$, 4) $I_S=30\text{ mA}$, $I_L=30\text{ mA}$.

- [1] W. Drexler, J. Biomedical Optics, **9**, 47 (2004).
- [2] M.A. Choma, M.V. Sarunic, C. Yang and J.A. Izatt, Opt. Expr., **11**, 2183 (2003).
- [3] S.H. Yun, C. Boudoux, J.F. de Boer, G.J. Tearney and B.E. Bouma, IEEE Phot. Tech Letts, **16**, 293 (2004).
- [4] R. Huber, M. Wojtkowski, J.G. Fujimoto, J.Y. Jian and A.E Cable, Opt. Expr., **13**, 10523 (2005).
- [5] H. Ishii, H. Tanobe, F. Kano, Y. Tohmori, Y. Kondo and Y. Yoshikuni, J. Quant. Elec., **32**, 433 (1996).
- [6] I.R. Sellers, H.Y. Liu, K.M. Groom, D.T. Childs, D. Robbins, T.J. Badcock, M. Hopkinson, D.J. Mowbray and M.S. Skolnick, Elec. Letts., **40**, 1412 (2004).
- [7] M. Sugawara, N. Hatori, M. Ishida, H. Ebe, Y. Arakawa, T. Akiyama, K. Otsubo, T. Yamamoto and Y. Nakata, J. Phys. D: Appl. Phys., **38**, 2126 (2005).